Isolation and Characterization of an Orthoreovirus from Indonesian Fruit Bats

Kittiya Intaruck[1], Yukari Itakura[1], Mai Kishimoto[1], Herman M Chambaro[1], Agus Setiyono[2], Ekowati Handharyani[2], Kentaro Uemura[1,3,4], Hayato Harima[5,#], Satoshi Taniguchi[6], Masayuki Saijo[6], Takashi Kimura[7], Yasuko Orba[1,8], Hirofumi Sawa[1, 5, 8, 9, 10], Michihito Sasaki[1]*

[1] Division of Molecular Pathobiology, International Institute for Zoonosis Control, Hokkaido University, Sapporo, Japan

[2] Department of Veterinary Clinic, Reproduction and Pathology, Faculty of Veterinary Medicine, IPB University, Bogor, Indonesia

[3] Drug Discovery and Disease Research Laboratory, Shionogi & Co., Ltd., Osaka, Japan

[4] Laboratory of Biomolecular Science, Faculty of Pharmaceutical Sciences, Hokkaido University, Sapporo, Japan

[5] Division of International Research Promotion, International Institute for Zoonosis Control, Hokkaido University, Sapporo, Japan

[6] Department of Virology 1, National Institute of Infectious Diseases, Tokyo, Japan

[7] Laboratory of Comparative Pathology, Faculty of Veterinary Medicine, Hokkaido University, Sapporo, Japan

[8] International Collaboration Unit, International Institute for Zoonosis Control, Hokkaido University, Sapporo, Japan

[9] One Health Research Center, Hokkaido University, Sapporo, Japan

[10] Global Virus Network, Baltimore, MD, USA

*Corresponding author: Michihito Sasaki, E-mail: m-sasaki@czc.hokudai.ac.jp

#Current affiliation: Laboratory of Veterinary Public Health, Faculty of Agriculture, Tokyo University of Agriculture and Technology, Tokyo, Japan

Abstract

Nelson Bay orthoreovirus (NBV) is an emerging bat-borne virus and causes respiratory tract infections in humans sporadically. Over the last two decades, several strains genetically related to NBV were isolated from humans and various bat species, predominantly in Southeast Asia (SEA), suggesting a high prevalence of the NBV species in this region. In this study, an orthoreovirus (ORV) belonging to the NBV species was isolated from Indonesian fruit bats' feces, tentatively named Paguyaman orthoreovirus (PgORV). Serological studies revealed that 81.2% (108/133) of Indonesian fruit bats sera had neutralizing antibodies against PgORV. Whole-genome sequencing and phylogenetic analysis of PgORV suggested the occurrence of past reassortments with other NBV strains isolated in SEA, indicating the dispersal and circulation of NBV species among bats in this region. Intranasal PgORV inoculation of laboratory mice caused severe pneumonia. Our study characterized PgORV's unique genetic background and highlighted the potential risk of PgORV-related diseases in Indonesia.

Keywords: Orthoreovirus; Nelson Bay orthoreovirus; Indonesia; Fruit bats; Virus isolation; Viral pathogenicity

Introduction

Nelson Bay orthoreovirus (NBV) is an emerging bat-borne virus that sporadically causes respiratory tract infection in humans [1–5]. The NBV prototype strain was isolated from the blood of a flying fox (*Pteropus poliocephalus*) collected in Nelson Bay, Australia, in 1968 and was designated as Nelson Bay virus [6]. NBV belongs to the genus *Orthoreovirus* (ORV) in the subfamily *Spinareovirinae*, the family *Reoviridae*. Ten species belong to this genus, including Mammalian orthoreovirus (MRV), Avian orthoreovirus (ARV), Nelson Bay orthoreovirus (NBV), Baboon orthoreovirus (BRV), Reptilian orthoreovirus (RRV), Mahlapitsi orthoreovirus (MAHLV), Piscine orthoreovirus (PRV), Broome orthoreovirus (BrRV), Neoavian orthoreovirus (NARV), and Testudine orthoreovirus (TRV). The common ORV characteristics include a non-enveloped, icosahedral shape consisting of ten linear double strand RNA segments with three large segments (L1–L3), three medium segments (M1–M3), and four small segments (S1–S4). ORV can be subdivided into fusogenic and non-fusogenic groups based on the ability to form multinucleated syncytial cells. Most ORV species, except for MRV and PRV, are fusogenics that encode the fusion-associated small transmembrane (FAST) protein influencing syncytial formation.

Bats serve as important natural reservoirs of several pathogens, including ORVs. MRV, NBV, and BrRV have been isolated from insectivorous and frugivorous bats [6–19]. Bat MRVs were mostly detected in insectivorous bats in Europe and China [7–10], while NBV species were found in fruit bats [6,11,12,14–19]. NBV species have been reported globally in Australia, Southeast Asia (SEA), China, and Africa [1–6,11,12,14–19]. Among 17 strains of NBV species discovered, 12 have been isolated from humans and various fruit bat species in Malaysia, Indonesia, and the Philippines, indicating NBV distribution in the SEA region [1–5,14,17–19]. Several NBV strains were isolated from patients with acute respiratory tract diseases who had previous history of close contact with bats or traveled to SEA countries, suggesting interspecies

transmission between bats and humans [1–5]. Additionally, NBV strains, Melaka virus (MelV) and Kampar virus (KamV), caused human-to-human transmission in Malaysia [4,5]. Consequently, NBV infection could cause respiratory disease in humans and is an emerging public health concern.

Indonesian fruit bats are carriers of many viruses, including herpesviruses, parvoviruses, polyomaviruses, paramyxoviruses, and coronaviruses [20–26]. Moreover, NBV infection incidence has been reported in four human cases in Indonesia [2,3]; however, knowledge about the prevalence of NBV in bats and humans in the country is insufficient. Previous studies established two members of NBV strains isolated from flying foxes (*Pteropus vampyrus*) captured in Indonesia, named Indonesia/2010 and Garut-69 [17,19]. Here we report a novel member of NBV species isolated from fruit bats in Indonesia, designated as Paguyaman orthoreovirus (PgORV). Viral characterization *in vitro* and *in vivo* suggested the possibility of genetic reassortment events with other NBV strains, and intranasal inoculation of laboratory mice with the isolated virus caused severe pneumonia. The serological examination revealed a high prevalence of NBV infection in Indonesian fruit bats.

Materials and Methods

Cells and viruses

Vero E6, BHK-21 (BHK), A549 cells were cultured and maintained in Dulbecco's Modified Eagle Medium (DMEM) with 10% fetal bovine serum (FBS). HEK293T (293T) cells were grown in high glucose DMEM with 10% FBS, and Caco-2 cells were cultured in a collagen-coated plate in DMEM supplemented with 10% FBS and 1% non-essential amino acid solution. Human serine protease TMPRSS2- stably expressing Vero E6 cells (Vero T2) were previously described [27]. NBV Miyazaki-Bali/2007 strain (MB) [2] was propagated in 293T cells, and the virus stock was titrated by plaque assay using Vero E6 cells.

93

94 ***Bat samples and ethics statements***

95 Blood, feces and organs were collected from fruit bats in eight areas of Indonesia
96 between 2010 and 2014 (Table 1). The samples were previously used for other virus screening
97 [20,21,23–26]. The Animal Care and Use Committee of Veterinary Teaching Hospital, IPB
98 University approved the protocol for bat sampling (permit number 05-2010 RSHP-IPB).
99 Collection and exportation of samples from fruit bats were performed under the permission of
100 the Directorate General of Livestock and Animal Health Services, Ministry of Agriculture,
101 Republic of Indonesia. As previously described, the bat species were identified by the external
102 morphology and the nucleotide sequence analysis of mitochondrial 16S RNA and *cytochrome*
103 *b* gene [26]. The Institutional Animal Care and Use Committee of Hokkaido University
104 approved the ethics for the viral inoculation to laboratory animal experiments (approval
105 number 20-0026).

106

107 ***Virus titration by plaque assay***

108 Confluent monolayer of Vero E6 in a 12 well plate was inoculated with a serially
109 diluted virus solution, and incubated for 1 hour for viral absorption. Then, the cells were
110 overlaid with DMEM containing 2% FBS and 0.4% agar. After three days post-inoculation
111 (dpi), the cells were fixed with 10% buffered formalin and stained with 1% crystal violet. The
112 viral titer was estimated as plaque-forming unit (pfu) based on the number of plaques.

113

114 ***Plaque reduction neutralization test (PRNT)***

115 Sera from a total of 133 Indonesian fruit bats were heat-inactivated at 56°C for 30 min
116 and serially diluted four-folds from 1: 10 to 1: 640. The diluted sera were mixed with an equal
117 volume of DMEM with 2% FBS containing 100–200-pfu of either MB or PgORV and

incubated for 1 hour at 37°C. The mixture of the virus and serum (100 μl) was subjected to a plaque assay using Vero E6 cells as described above. Neutralizing antibody titers were determined as the highest dilution, which achieved more than 80% reduction in plaque numbers.

Screening of the ORV genome by nested RT-PCR

Total RNA was extracted from feces using a High Pure Viral Nucleic Acid Kit (Roche Diagnostics, Mannheim, Germany). Lungs were homogenized in TRIzol reagent (Invitrogen; Thermo Scientific, Waltham, USA) and subjected to RNA extraction using a Direct-Zol RNA MiniPrep kit (Zymo Research, Irvine, USA). The RNA samples were subjected to ORV screening by nested RT-PCR using two sets of degenerate primers targeting the ORV RNA-dependent RNA polymerase (RdRp) gene as described previously [28]. The first round RT-PCR was performed using 1607F primer (5′-CARMGNCGNSCHMGHTCHATHATGCC-3′), 2608R primer (5′-TAVAYRAAVGWCCASMHNGGRTAYTG-3′) and PrimeScript OneStep RT-PCR Kit Ver.2 (Takara Bio, Kusatsu, Japan). The second round PCR was performed with 2090F primer (5′-GGBTCMACNGCYACYTCBACYGAGCA-3′), 2334R primer (5′-CDATGTCRTAHW YCCANCCRAA-3′) and TaKaRa ExTaq Hot Start Version (Takara Bio). Amplicons at approximately 300 bp were subjected to sequencing using Big Dye Terminator v3.1 Cycle Sequencing Kit (Applied Biosystems; Thermo Scientific).

Virus isolation

Fecal samples positive for the ORV genome were suspended in phosphate buffer saline (PBS) at 10% w/v. The suspensions were inoculated onto Vero T2 cells. Cells were maintained in serum-free DMEM supplemented with 2% antibiotic-antimycotic solution (Wako, Osaka, Japan), gentamicin (25 μg/ml), and trypsin (0.5 μg/ml). The culture supernatant was passaged

into fresh monolayer cells after 5-dpi. The supernatants from wells showing a cytopathic effect (CPE) were harvested and maintained at −80°C as a master stock of isolated viruses.

Whole-genome sequencing

Total RNA was extracted from five viral clones (ORV13-7, ORV13-8, ORV13-20, ORV13-25, and ORV13-27) and transcribed into double-stranded cDNA using PrimeScript Double Strand cDNA Synthesis Kit (Takara Bio). The sequence library was constructed using Nextera XT DNA Library Preparation Kit and sequenced on an Illumina MiSeq instrument (Illumina, San Diego, USA). The obtained sequence reads were assembled into contigs via *de novo* assembly or mapped to reference genome segments of MB strain (GenBank accession; AB908278-AB908287) using CLC Genomics Workbench 20.1 (Qiagen, Hilden, Germany) and Geneious 2021.1.1 software (Biomatters, Newark, USA). Nucleotide sequences of ORV13-27 segments were deposited in DDBJ with the accession numbers LC632072-LC632081.

Phylogenetic analysis

Reference nucleotide sequences of NBV species were obtained from the GenBank database and aligned with PgORV sequences. The best fit mathematical models for phylogenetic analyses of each segment were determined using MEGA7 software [29]. Phylogenetic trees were constructed using the maximum likelihood method with 1,000 bootstrap replicates.

Replication efficiency in different cell lines

BHK, Vero E6, Vero T2, A549, Caco-2, and 293T cells were inoculated with PgORV (ORV13-27) at two different multiplicities of infection per cell (MOI = 0.01 or 0.0001) and

maintained in culture media containing 2% FBS. Cell culture supernatants containing progeny viruses were harvested at 8, 24, 48, and 72 hours post-infection (hpi), and titrated by a plaque assay using Vero E6 cells.

Immunofluorescence assay (IFA)

Cells were seeded in a 24-well plate before inoculation with PgORV (ORV13-27, MOI = 0.01 or 0.0001). Cells were fixed with 10% buffered formalin at 14-hpi and permeabilized with 0.5% Triton X-100 in PBS. After blocking with 50% Block Ace (KAC, Kyoto, Japan), cells were incubated with guinea pig anti-NBV Nachunsulwe-57 polyclonal antibody, which cross-reacted with PgORV [15] (Supplementary Figure S1) and Alexa 488-conjugated goat anti-guinea pig IgG (Invitrogen) as a secondary antibody. Cell nuclei were stained with Hoechst 33342 (Invitrogen) and the fluorescence signal was examined using a fluorescence microscope (IX73; Olympus, Tokyo, Japan).

Animal experiments

Male BALB/c mice (4–6 week-old, Japan SLC, Hamamatsu, Japan) were intranasally inoculated with PgORV (1×10^6 pfu of ORV13-27 in 50 µl PBS) or mock (50 µl PBS). Body weight (BW) was monitored daily up to 14-dpi and 20% BW loss was defined as a humane endpoint. To evaluate PgORV's growth and pathogenicity in laboratory mice, the lung was harvested at 1, 3, and 5-dpi for viral load measurement (n = 5) and histopathological examination (n = 3).

Measurement of the viral RNA load and cytokine gene expression in lung tissue

The lungs from mice experimentally infected with PgORV were homogenized in PBS at 10% w/v using TissueRuptor (Qiagen). Total RNA was extracted from the lung homogenates

with TRIzol LS reagent and Direct-Zol RNA MiniPrep kit. qRT–PCR assay was conducted using OneStep PrimeScript III RT–qPCR Mix (Takara Bio) with the primers and probe targeting the L1 segment of NBV species as described previously [30], TaqMan mouse β-actin Endogenous Control (Mm00607939_s1, Applied Biosystems) or predesigned PrimeTime qPCR Assays for TNF (Ms.PT.58.12575861), IFN-γ (Ms.PT.58.41769240), IFN-β (Ms.PT.30132453.g), IL-6 (Ms.PT.58.10005566), CCL2 (Ms.PT.58.42151692) and CXCL10 (Ms.PT.58.43575827) (IDT, Coralville, USA). The levels of viral RNA and cytokine gene expression were normalized to β-actin and calculated the relative gene expression using $2^{-\Delta Ct}$ or $2^{-\Delta\Delta Ct}$ method [31].

Histopathology and immunohistochemistry (IHC)

Lungs from the PgORV-inoculated mice were fixed in 10% buffered formalin, embedded in paraffin blocks, and sectioned at 4 μm. The sections were stained with Hematoxylin and Eosin for histopathological examination. To detect PgORV antigen in lungs, the sections were deparaffinized and heated for three minutes in citrate buffer for antigen retrieval. The slides were blocked with 50% Block Ace and incubated with guinea pig anti-NBV Nachunsulwe-57 polyclonal antibody [15]. Immunostaining was visualized using VECTASTAIN ABC guinea pig IgG Kit (Vector laboratories, Burlingame, USA) and Histofine diaminobenzidine substrate kit (Nichirei Biosciences, Tokyo, Japan).

Statistical analysis

Data were analyzed and presented as the mean with standard deviation (SD). Statistical analysis was performed using Prism 8 (GraphPad Software, San Diego, USA). Survival analysis was performed using Kaplan-Meier estimator. One-way ANOVA with Dunnett's test

was used to determine the statistical significance of cytokine gene expression in the mouse lungs.

Results

Screening and isolation of orthoreovirus in Indonesian fruit bats

To estimate NBV infection among fruit bats in Indonesia, the neutralizing activity of fruit bat serum samples to NBV MB strain by PRNT was examined. Among 133 serum samples, 118 (89.5%) had neutralizing activity against MB (1: 20 to 1: 1,280) (Table 1). Seropositive bats were identified from *Pteropus vampyrus* (47/47), *Pteropus* sp. (42/42), *Dobsonia moluccensis* (16/16), and *Acerodon celebensis* (14/28) (Table 1). ORV genome in feces (96) and lungs (172) from fruit bats was also examined by nested RT-PCR. The ORV genome was detected in the feces from *Pteropus* sp. (3/8) and *Acerodon celebensis* (3/7) collected in 2013, but not in the lungs (Table 1). Sequence analysis and BLAST search showed that the amplicons had high nucleotide sequence identity to the RdRp gene of NBV species.

Next, we attempted to isolate ORV from bat feces. Six fecal suspensions positive for the ORV genome were inoculated into Vero T2 cells. Finally, five of six inocula (Sample ID: 13-7, 13-8, 13-20, 13-25, and 13-27) induced CPE and syncytium formation in cells, characteristic of fusogenic ORV infection. After the first passage, five viral clones from sample ID: 13-7, 13-8, 13-20, 13-25, and 13-27 were successfully isolated. It was confirmed that isolated viruses were ORVs using RT-PCR and nucleotide sequencing of the ORV RdRp gene. The information of five bat samples positive for virus isolation is shown in Supplementary Table S1.

Whole-genome sequencing and phylogenetic analysis

We conducted complete genome sequencing of the five isolated ORVs (designated as ORV13-7, ORV13-8, ORV13-20, ORV13-25, and ORV13-27). Sequence comparison of the five viral clones displayed more than 99% nucleotide identity, indicating that all clones were the same virus strain. The isolated virus was designated as Paguyaman orthoreovirus (PgORV) based on where the bat carrying the virus was captured (Supplementary Table S1).

ORV13-27 was chosen from the five clones as a representative PgORV clone for further characterization. The complete PgORV genome was 23,406 bp in total length, and the lengths of the ten segments are shown in Table 2. Sequence analysis demonstrated that PgORV had the same genome organization as other NBV strains. All the segments except for S1 encode only one protein (monocistronic), but the PgORV S1 segment encodes three viral proteins (tricistronic) (Table 2). The terminal sequences of the 5′-untranslated region (5′-UTR) and the 3′-UTR of the segments (GCUUhh and UCAUC, respectively) were conserved among the genus *Orthoreovirus*. BLAST search revealed that L1, L3, M1–M3, and S4 segments shared the highest nucleotide sequence identities with those of MB (Table 2). Phylogenetic analysis showed that S1 was the most genetically divergent among the segments (Figure 1A). The PgORV-S1 segment shared the same ancestor with NBVs from human patients in Malaysia (Sikamat and Melaka) and NBVs from macaques in Thailand (Lopburi 01 and Lopburi 02) [1,5,32]. L1, L3, M1, M2, M3 and S4 segments of PgORV formed clusters with MB and other NBV strains originated in Indonesia, including Indonesia/2010, Garut-69, HK23629/07 (HK/07), HK46886/09 (HK/09), and HK50842/10 (HK/10) strains (Figure 1B) [2,3,17,19]. Conversely, L2, S2, and S3 segments of PgORV were closely related to Talikud and Samal strains isolated from bats in the Philippines [14]. L2 and S3 displayed 89.1% and 93.6% nucleotide sequence identity with Talikud-74 and Samal-24, respectively, while the nucleotide sequence of the S2 segment was highly similar to the prototype NBV (89.6% identity).

Seroprevalence of PgORV in Indonesian fruit bats

The neutralizing activity of fruit bat serum samples to PgORV infection was evaluated using PRNT. The results showed that 81.2% (108/133) of bat sera were positive for PgORV infection neutralization, and the seropositive rate was slightly lower than that of MB (89.5%) (Table 1 and Table 3). Most bat sera showed neutralizing activity against both PgORV and MB, suggesting a possible cross-neutralization between these NBV members (Supplementary Figure S2). However, 57.9% (77/133) of bat sera exhibited a higher neutralizing titer against MB than PgORV.

Growth properties of PgORV in cell lines

Using several cell lines, we characterized the infectivity and growth kinetics of PgORV *in vitro*. For the immunofluorescence staining of the PgORV antigen, convalescent serum from a guinea pig infected with NBV Nachunsulwe-57 strain was employed as a primary antibody [15]. IFA analysis showed that all examined cell lines were susceptible to the infection with PgORV at an MOI of 0.01 (Figure 2A). Morphologically, distinct syncytia formations were observed in BHK, Vero E6, and Vero T2 cells, but almost all cells were infected and formed huge syncytia in Caco-2 and 293T cells. In A549 cells, some cells detached from the culture plates at 14-hpi. The virus titers in BHK supernatants, Vero E6 and Vero T2 cells, increased over time (Figure 2B). Contrastly, the virus titers in A549, Caco-2, and 293T cells peaked at 24 or 48-hpi, presumably due to CPE and cell detachment by PgORV infection. To observe multiple cycles of viral infection in A549, Caco-2, and 293T cells, cells were inoculated with PgORV at a MOI of 0.0001. Infected cells were scarcely observed in BHK, Vero E6, and Vero T2 cells, but A549, 293T, and Caco-2 cells were highly sensitive to the infection even at the lower MOI (Figure 2C). The virus titers in the supernatants of A549, 293T, and Caco-2 cells

290 also time-dependently increased, and the 293T cells had the highest progeny virus production
291 (Figure 2D).
292
293 ***Pathogenicity of PgORV in laboratory mice***
294 To investigate PgORV pathogenicity, we inoculated BALB/c mice *via* the intranasal
295 route with 1×10^6 pfu virus. The mice were monitored for BW and sacrificed for viral titer and
296 histopathological changes in the lungs (Figure 3A). The mice BW continuously decreased from
297 1-dpi to 4-dpi PgORV and then turned to recovery (Figure 3B). Five of eight mice inoculated
298 with PgORV reached an endpoint due to severe BW loss (>20%) at 4-dpi and 6-dpi (Figure
299 3C). The other three mice recovered and survived the infection. The viral titer and viral RNA
300 level in the lung were quantified using plaque assay and qRT–PCR, respectively. The peak of
301 viral titer was observed in the lung of mice at 1-dpi PgORV, and the titer decreased time-
302 dependently (Figure 3D). Similarly, the viral RNA load was also the highest at 1-dpi and
303 gradually decreased (Figure 3E).
304 Additionally, histopathological changes in the lungs after PgORV inoculation was
305 examined. Macroscopically, the lungs of mice inoculated with PgORV exhibited hyperemia at
306 3 and 5-dpi (Figure 4A). Histopathological examination revealed hemorrhage and infiltration
307 of inflammatory cells in lungs at 1, 3, and 5-dpi, and massive infiltration of inflammatory cells
308 was observed at 5-dpi (Figure 4B). Viral antigens were detected in bronchial and alveolar
309 epithelial cells at 1 and 3-dpi using IHC; however, little IHC signal was detected at 5-dpi
310 (Figure 4C). Pneumonia severity correlated conversely with decreased viral load, as indicated
311 by IHC, qRT–PCR, and plaque assay. These results imply that the host immune response to
312 the infection eliminated the virus in the lung but caused severe inflammation.
313 To investigate the host immune responses against PgORV infection, we examined the
314 expression levels of inflammatory cytokine genes in PgORV-inoculated mice lungs using

qRT–PCR. The levels of pro-inflammatory cytokines, including TNF, IFN-β, and IL-6 as well as chemoattractants (CCL2 and CXCL2), were significantly increased in PgORV-infected mice lungs at 1-dpi, indicating the early host responses to viral infection. Contrastly, IFN-γ, which influences viral clearance, was significantly upregulated in mice lungs at 5-dpi (Figure 4D), supporting the hypothesis of the viral clearance by host immune responses in mice.

Discussion

Since NBV discovery, several NBV strains have been identified from fruit bats [6,11,12,14–19]. Approximately 75% of NBV strains were isolated in SEA countries, indicating a high NBV prevalence in this region. Currently, six NBV strains, including HK/07, HK/09, HK/10, MB, Indonesia/2010, and Garut-69, have been reported in Indonesia [2,3,17,19]. Three HK strains and MB were isolated from the respiratory tract specimens of patients who had a history of visiting Bali, Indonesia, before the onset [2,3]. Garut-69 was isolated from *Pteropus vampyrus* in West Java Island [19]; however, there was no information on sampling sites of bats from which Indonesia/2010 was detected [17]. In this study, we detected NBV seropositive bats from West Sumatra (Lima Puluh Kota), West Java (Panjalu, Magelang, and Surabaya), North Sulawesi (Popayato and Paguyaman), and South Sulawesi (Soppeng and Sidrap), indicating the broad NBV infection dispersal among Indonesian fruit bats.

L1, L3, M1, M2, M3, and S4 segments of PgORV showed high nucleotide sequence identities (93.4%–98.2%) with MB, suggesting that PgORV and MB evolved from a common ancestor. However, the remaining L2, S1, S2, and S3 segments of PgORV were phylogenetically distant from those of MB and related to other NBVs. This phylogenetic incongruence suggests genetic reassortments between NBVs in fruit bats, reported in several studies [12,14,16,17,19,32]. The fact that bats can fly long distances and move between islands

and countries may contribute to a long-distance dispersal and genetic reassortment of ORVs [33–35]. Although multiple NBV strains were isolated from SEA countries, we could not recognize clear relationship between phylogeny and geographic distribution of NBVs (Figure 1).

Previous studies reported that 23, 83, and 98% of fruit bats were NBV seropositive in China, the Philippines, and Zambia, respectively [14–16]. Similarly, this study revealed that 81.2–89.5% of Indonesian fruit bat sera had neutralizing antibodies against NBV. Bats are highly diversified with over 1,400 species worldwide and almost 200 species of fruit bats. Various fruit bat species, including *Pteropus poliocephalus*, *Pteropus hypomelanus*, *Rousettus leschenautia*, *Rousettus amplexicaudatus*, *Rousettus aegyptiacus*, *Eonycteris spelaea*, *Macroglossus minimus*, *Lissonycteris angolensis ruwenzorii,* and *Eidolon helvum,* were evidenced for NBV infections [6,11,12,14–19]. Here, we showed the NBV-seroprevalence in *Acerodon celebensis* and *Dobsonia moluccensis*. In addition, we have identified PgORV from fruit bats belonging to two different genera (*Pteropus sp.* and *Acerodon celebensis*). Other study also isolated NBVs with almost identical genome sequences from *Eonycteris spelaea* and *Rousettus amplexicaudatus* [14]. Collectively, these findings suggest that at least some NBVs broadly distribute among fruit bats with frequent interspecies transmissions.

Our PRNT assay revealed a high seropositivity rate for both NBVs, PgORV, and MB in Indonesian fruit bats. Among NBV members, PgORV was phylogenetically close to MB; therefore, it was supposed that the antibodies could cross-react with both NBVs. Cross-neutralization has been observed in several strains of NBV species. Antisera to the prototype NBV cross-reacts with Pulau (PuV), MelV, and KamV [4]. Antisera against MB has also showed the cross-reactivity to NBVs of Samal-24 and Talikud-82 [14]. Neutralizing antibodies against Nachunsulwe-57 cross-reacted with MB [15]. Additionally, our PRNT assays showed that a subset of bat sera exhibited higher neutralizing activity to MB strain than PgORV,

365 suggesting that these bats would be exposed to MB or MB-related NBV rather than PgORV.
366 For these reasons, we cannot exclude the possibility of cross-reactivity between PgORV and
367 known/unknown NBV members in our PRNT assay.

368 After replication in host cells, the virus spreads to adjacent cells via two modes; cell-
369 free and cell-to-cell transmissions [36–38]. The multinuclear syncytium is a characteristic of
370 cells infected with PgORV. The IFA detected the syncytia with PgORV antigen in BHK, Vero
371 E6, and Vero T2 cells at 14-hpi. However, the progeny virus titers in the culture supernatant
372 of these cell lines were under the detection limit at 24-hpi. These results suggest that the
373 primary main PgORV spreading mode is cell-to-cell mechanism. Similar to MB, Samal-24,
374 and Garut-50 [14,39], human A549, Caco-2, and 293T cells, were highly susceptible to PgORV
375 infection. Although we employed Vero T2 for virus isolation, using A549, Caco-2, and 293T
376 cells could be a better outcome for NBV isolation.

377 The mortality rate of PgORV-inoculated mice (62.5%) was lower than that of MB-
378 inoculated mice (100%), indicating that MB is more pathogenic than PgORV in mice [40,41].
379 As with the case of MB and Samal-24 [40], PgORV infection caused severe pneumonia in mice
380 lungs. Hemorrhage and infiltration of inflammatory cells were massively present in the lungs
381 at 3 and 5-dpi, while cells positive for viral antigen were abundant at 1-dpi and subsequently
382 decreased at 3 and 5-dpi, indicating PgORV clearance from the host. The manifestation of
383 PgORV-infected mice was uncorrelated with the viral load in the lungs. This discrepancy is
384 observed in mouse models infected with influenza, respiratory syncytial, and corona viruses
385 [42–44]. The expression levels of pro-inflammatory cytokines (TNF, IFN-β1, and IL-6) and
386 chemoattractants (CCL2 and CXCL10) were significantly upregulated at 1-dpi for the initial
387 responses to viral infection, and subsequent recruitment of inflammatory cells causing IFN-γ
388 expression induction. TNF and IFN-γ influence virus clearance and cause immunopathology
389 [45,46].

In conclusion, we isolated PgORV from fruit bats, which can cause respiratory disease in mammals. We also demonstrated a high seroprevalence of NBV in multiple species of fruit bats in different areas of Indonesia. Our study emphasizes the broad distribution and circulation of NBV among fruit bats in Indonesia. Further investigations in bats, other animals, and humans should be conducted to evaluate the current burden of NBV infections in Indonesia.

Acknowledgements

This study was supported in part by the Japan Society for the Promotion of Science (JSPS) KAKENHI under grant numbers 21K19619 and 21K05951; Japan Science and Technology Agency (JST) Moonshot R&D under grant number JPMJMS2025; and the World-leading Innovative and Smart Education (WISE) Program from the Ministry of Education, Culture, Sports, Science, and Technology (MEXT), Japan under grant number 1801.

Declaration of interest statement

K.U. is an employee of Shionogi & Co., Ltd. The authors declare no competing interests.

References

1 Chua KB, Voon K, Yu M, *et al.* Investigation of a potential zoonotic transmission of orthoreovirus associated with acute influenza-like illness in an adult patient. PLoS One 2011; 6: e25434.

2 Yamanaka A, Iwakiri A, Yoshikawa T, *et al.* Imported case of acute respiratory tract infection associated with a member of species nelson bay orthoreovirus. PLoS One 2014; 9: e92777–e92777.

3 Wong AH, Cheng PKC, Lai MYY, *et al.* Virulence potential of fusogenic orthoreoviruses. Emerg Infect Dis 2012; 18: 944–948.

4 Chua KB, Voon K, Crameri G, *et al.* Identification and characterization of a new orthoreovirus from patients with acute respiratory infections. PLoS One 2008; 3: 1–7.

5 Chua KB, Crameri G, Hyatt A, *et al.* A previously unknown reovirus of bat origin is associated with an acute respiratory disease in humans. Proc Nalt Acad Sci USA 2007; 104: 11424.

6 Gard G, Compans RW. Structure and cytopathic effects of Nelson Bay Virus. J Virol 1970; 6: 100-106.

7 Lelli D, Moreno A, Lavazza A *et al.* Identification of Mammalian Orthoreovirus Type 3 in Italian Bats. Zoonoses and Public Health 2013; 60: 84–92.

8 Wang L, Fu S, Cao L *et al.* Isolation and Identification of a Natural Reassortant Mammalian Orthoreovirus from Least Horseshoe Bat in China. PLoS One 2015; 10: e0118598.

9 Kohl C, Lesnik R, Brinkmann A, *et al.* Isolation and characterization of three mammalian orthoreoviruses from European bats. PLoS One 2012; 7: e43106.

10 Naglič T, Rihtarič D, Hostnik P, *et al.* Identification of novel reassortant mammalian orthoreoviruses from bats in Slovenia. BMC Vet Res 2018; 14: 264.

11 Du L, Lu Z, Fan Y, *et al.* Xi River virus, a new bat reovirus isolated in southern China. Arch Virol 2010; 155: 1295–1299.

12 Bennett AJ, Goldberg TL. Pteropine orthoreovirus in an Angolan soft-furred fruit bat (*Lissonycteris angolensis*) in Uganda dramatically expands the global distribution of an emerging bat-borne respiratory virus. Viruses 2020; 12. doi:10.3390/v12070740.

13 Thalmann CM, Cummins DM, Yu M *et al.* Broome virus, a new fusogenic Orthoreovirus species isolated from an Australian fruit bat. Virology 2010; 402: 26–40.

14 Taniguchi S, Maeda K, Horimoto T, *et al.* First isolation and characterization of pteropine orthoreoviruses in fruit bats in the Philippines. Arch Virol 2017; 162: 1529–1539.

15 Harima H, Sasaki M, Orba Y, *et al.* Attenuated infection by a pteropine orthoreovirus isolated from an Egyptian fruit bat in Zambia. PLoS Negl Trop Dis 2021; 15: e0009768.

16 Hu T, Qiu W, He B, *et al.* Characterization of a novel orthoreovirus isolated from fruit bat, China. BMC Microbiol 2014; 14: 293.

17 Lorusso A, Teodori L, Leone A, *et al.* A new member of the pteropine orthoreovirus species isolated from fruit bats imported to Italy. Infect Genet Evol 2015; 30: 55–58.

18 Pritchard LI, Chua KB, Cummins D, *et al.* Pulau virus; a new member of the Nelson Bay orthoreovirus species isolated from fruit bats in Malaysia. Arch Virol 2006; 151: 229–239.

19 Takemae H, Basri C, Mayasari NLPI, *et al.* Isolation of pteropine orthoreovirus from *Pteropus vampyrus* in Garut, Indonesia. Virus Genes 2018; 54: 823–827.

20 Sasaki M, Setiyono A, Handharyani E, *et al.* Isolation and characterization of a novel alphaherpesvirus in fruit bats. J Virol 2014; 88: 9819–9829.

21 Wada Y, Sasaki M, Setiyono A, *et al.* Detection of novel gammaherpesviruses from fruit bats in Indonesia. J Med Microbiol 2018; 67: 415–422.

22 Sendow I, Ratnawati A, Taylor T, *et al*. Nipah virus in the fruit bat *Pteropus vampyrus* in Sumatera, Indonesia. PLoS One 2013; 8. doi:10.1371/journal.pone.0069544.

23 Kobayashi S, Sasaki M, Nakao R, *et al.* Detection of novel polyomaviruses in fruit bats in Indonesia. Arch Virol 2015; 160: 1075–1082.

24 Sasaki M, Gonzalez G, Wada Y, *et al.* Divergent bufavirus harboured in megabats represents a new lineage of parvoviruses. Sci Rep 2016; 6. doi:10.1038/srep24257.

25 Anindita PD, Sasaki M, Setiyono A, *et al.* Detection of coronavirus genomes in Moluccan naked-backed fruit bats in Indonesia. Arch Virol 2015; 160: 1113–1118.

26 Sasaki M, Setiyono A, Handharyani E, *et al.* Molecular detection of a novel paramyxovirus in fruit bats from Indonesia. Virol J 2012; 9: 240.

27 Sasaki M, Uemura K, Sato A *et al.* SARS-CoV-2 variants with mutations at the S1/S2 cleavage site are generated in vitro during propagation in TMPRSS2-deficient cells. PLoS Pathog 2021; 17: e1009233.

28 Wellehan JFX, Childress AL, Marschang RE, *et al.* Consensus nested PCR amplification and sequencing of diverse reptilian, avian, and mammalian orthoreoviruses. Vet Microbiol 2009; 133: 34–42.

29 Kumar S, Stecher G, Tamura K. MEGA7: Molecular Evolutionary Genetics Analysis Version 7.0 for Bigger Datasets. Mol Biol Evol 2016; 33: 1870–1874.

30 Kanai Y, Kawagishi T, Sakai Y, *et al.* Cell-cell fusion induced by reovirus FAST proteins enhances replication and pathogenicity of non-enveloped dsRNA viruses. PLoS Pathog 2019; 15. doi:10.1371/journal.ppat.1007675.
31 Livak KJ, Schmittgen TD. Analysis of Relative Gene Expression Data Using Real-Time Quantitative PCR and the $2^{-\Delta\Delta CT}$ Method. Methods 2001; 25: 402–408.
32 Kosoltanapiwat N, Reamtong O, Okabayashi T, *et al.* Mass spectrometry-based identification and whole-genome characterisation of the first pteropine orthoreovirus isolated from monkey faeces in Thailand. BMC Microbiol 2018; 18. doi:10.1186/s12866-018-1302-9.
33 Breed AC, Field HE, Smith CS, Edmonston J, Meers J. Bats Without Borders: Long-Distance Movements and Implications for Disease Risk Management. EcoHealth 2010; 7: 204–212.
34 Kimprasit T, Nunome M, Iida K *et al.* Dispersal history of *Miniopterus fuliginosus* bats and their associated viruses in east Asia. PLoS One 2021; 16: e0244006.
35 Randhawa N, Bird BH, Van Wormer E *et al.* Fruit bats in flight: a look into the movements of the ecologically important *Eidolon helvum* in Tanzania. One Health Outlook 2020; 2: 16.
36 Cifuentes-Muñoz N, Dutch RE, Cattaneo R. Direct cell-to-cell transmission of respiratory viruses: The fast lanes. PLoS Pathog 2018; 14. doi:10.1371/journal.ppat.1007015.
37 Marsh M, Helenius A. Virus Entry: Open Sesame. Cell 2006; 124: 729–740.
38 Zhong P, Agosto LM, Munro JB, Mothes W. Cell-to-cell transmission of viruses. Curr Opin Virol 2013; 3: 44–50.
39 Tarigan R, Katta T, Takemae H, *et al.* Distinct interferon response in bat and other mammalian cell lines infected with pteropine orthoreovirus. Virus Genes 2021; 57: 510–520.
40 Egawa K, Shimojima M, Taniguchi S, *et al.* Virulence, pathology, and pathogenesis of pteropine orthoreovirus (PRV) in BALB/c mice: Development of an animal infection model for PRV. PLoS Negl Trop Dis 2017; 11: e0006076–e0006076.
41 Kanai Y, Kawagishi T, Okamoto M, *et al*. Lethal murine infection model for human respiratory disease-associated pteropine orthoreovirus. Virology 2018; 514: 57–65.
42 Myers MA, Smith AP, Lane LC, *et al.* Dynamically linking influenza virus infection kinetics, lung injury, inflammation, and disease severity. eLife 2021; 10. doi:10.7554/eLife.68864.
43 Ostler T, Davidson W, Ehl S. Virus clearance and immunopathology by $CD8^+$ T cells during infection with respiratory syncytial virus are mediated by IFN-γ. Eur J Immunol 2002; 32: 2117-2123.
44 Winkler ES, Bailey AL, Kafai NM *et al.* SARS-CoV-2 infection of human ACE2-transgenic mice causes severe lung inflammation and impaired function. Nat Immunol 2020; 21: 1327–1335.
45 Morris DR, Ansar M, Qu Y, *et al.* Combined blockade of IFN-Type I and TNF alpha receptors provides protection against respiratory syncytial virus (RSV)-induced disease and bronchoconstriction. J Immunol 2021; 206: 20.14.
46 Karki R, Sharma BR, Tuladhar S *et al.* Synergism of TNF-α and IFN-γ Triggers Inflammatory Cell Death, Tissue Damage, and Mortality in SARS-CoV-2 Infection and Cytokine Shock Syndromes. Cell 2021; 184: 149-168.e17.

Figure legend

Figure 1. Phylogenetic analysis of Paguyaman orthoreovirus (PgORV).

(A and B) Nucleotide sequences of 10 genome segments (L1-L3, M1-M3 and S1-S4) of reference orthoreoviruses and PgORV were aligned. Phylogenetic trees of S1 segment (A) and other segments (B) were constructed using the maximum likelihood method. Bootstrap values of 1,000 replicates are shown in each node and the scale bars represent the number of nucleotide substitutions per site. The host which the virus was identified, is shown in the phylogenetic tree of S1 segment (A). Each color indicates the country where the virus was identified (A and B).

Figure 2. Infectivity and growth of PgORV in cell lines.

Detection of PgORV infection by immunofluorescence staining (A, C). Cells were inoculated with the virus at multiplicities of infection (MOIs) of 0.0001 and 0.01 and fixed at 14 hours post infection. The cells were stained with guinea pig anti-NBV (Nachunsulwe-57) polyclonal antibody for PgORV (green) and Hoechst 33342 for cell nucleus (blue) (scale bars: 500 μm). (B, D) Cells were inoculated with PgORV at MOIs of 0.0001 and 0.01. Virus titers in cell culture supernatants at the indicated time points were determined by plaque assay.

Figure 3. Infection of laboratory mice with PgORV. (A) Scheme of experimental infection in BALB/c mice. Mice were intranasally infected with 1×10^6 pfu of PgORV or PBS as control. (B) The average percentage of body weight changes of mice after PgORV infection. (C) Survival rate of mice infected with PgORV. A humane endpoint was applied when the mice showed more than 20% body weight loss. (D) Virus titer in the lung at the indicated time points were determined by plaque assay. (E) Viral RNA levels in the lungs were

normalized to the mRNA levels of mouse β-actin (ACTB) and the relative expression of L1 gene was calculated by $2^{-\Delta Ct}$ method.

Figure 4. Pathological change and cytokine expression profile in the lung of mice infected with PgORV. BALB/c mice were infected intranasally with 1×10^6 pfu of PgORV. (A) Macroscopic appearances of mice lungs after infection. (B) Hematoxylin and Eosin (H&E) staining of the lung sections. (C) Detection of PgORV antigen in the lungs by immunohistochemistry. Lung sections were stained with guinea pig anti-NBV (Nachunsulwe-57) polyclonal antibody and counterstained of cell nuclei with Hematoxylin. Scale bars of the left panels (a, c, e, g): 200 μm, right panels (b, d, f, h): 50 μm. (D) Cytokine expression levels in the mice lungs. Data were normalized to β-actin and the relative gene expression level of each cytokine was calculated by $2^{-\Delta\Delta Ct}$ method. One-way ANOVA with Dunnett's test was used to determine the statistical significance of differences between uninfected control and infected mice. *, $p < 0.05$; **, $p < 0.01$, ***, $p < 0.001$; ****, $p < 0.0001$.

544 **Table 1.** Screening of neutralizing antibody against NBV Miyazaki-Bali/2007 strain and

545 ORV genome in Indonesian fruit bats

Year	Location	Bat species	Number of positive samples						
			Neutralizing antibody titer by $PRNT_{80}$					Nested RT-PCR	
			1:20	1:80	1:320	1:1280	Total (%)	Feces	Lung
2010	Panjalu	*Pteropus vampyrus*	1	5	7	2	15/15 (100)	NA[a]	0/15
2011	Lima Puluh Kota	*Pteropus vampyrus*	0	4	4	2	10/10 (100)	NA	0/20
	Paguyaman	*Pteropus* sp.[b]	4	4	5	5	18/18 (100)	NA	0/23
	Popayato	*Pteropus* sp.	0	0	1	2	3/3 (100)	NA	0/4
2012	Paguyaman	*Dobsonia moluccensis*	0	7	6	3	16/16 (100)	0/17	0/17
		Acerodon celebensis	2	4	2	1	9/18 (50)	0/18	0/18
		Pteropus sp.	0	0	2	0	2/2 (100)	0/2	0/2
	Surabaya	*Pteropus vampyrus*	0	1	0	2	3/3 (100)	0/3	0/3
	Magelang	*Pteropus vampyrus*	3	3	5	8	19/19 (100)	0/19	0/20
2013	Paguyaman	*Pteropus* sp.	0	1	6	3	10/10 (100)	3/8	0/10
		Acerodon celebensis	2	2	1	0	5/10 (50)	3/7	0/18
2014	Soppeng	*Pteropus* sp.	0	0	3	3	6/6 (100)	0/7	0/7
	Sidrap	*Pteropus* sp.	0	0	1	2	3/3 (100)	0/15	0/15
Total			**12**	**31**	**43**	**33**	**119/133 (89.5)**	**6/96**	**0/172**

546 [a]NA; sample not available, [b]*Pteropus* sp.; Bat genetically closely related to *Pteropus*

547 *hypomelanus.*

548 **Table 2.** Molecular characteristics of orthoreovirus isolated from Indonesian fruit bat

549 (ORV13-27).

Genome segment	Accession No.	Size (bp)	Terminal sequences		Encoded protein(s)	Closest strain (% nucleotide identity)
			5' UTR	3' UTR		
L1	LC632072	3896	GCUUUA	UCAUC	λC	Miyazaki-Bali/2007 (98.2)
L2	LC632073	3832	GCUUUA	UCAUC	λB	Talikud-74 (89.1)
L3	LC632074	3954	GCUUUA	UCAUC	λA	Miyazaki-Bali/2007 (93.4)
M1	LC632075	2295	GCUUUA	UCAUC	μA	Miyazaki-Bali/2007 (94.7)
M2	LC632076	2145	GCUUAU	UCAUC	μB	Miyazaki-Bali/2007 (96.5)
M3	LC632077	1984	GCUUAU	UCAUC	μNS	Miyazaki-Bali/2007 (96.4)
S1	LC632078	1602	GCUUAA	UCAUC	p10, p17, σC	Sikamat (84.5)
S2	LC632079	1322	GCUUAA	UCAUC	σA	Nelson bay virus (89.6)
S3	LC632080	1192	GCUUAU	UCAUC	σNS	Samal-24 (93.6)
S4	LC632081	1184	GCUUAU	UCAUC	σB	Miyazaki-Bali/2007 (96.6)

550

551

552 **Table 3.** Neutralizing antibody against PgORV in Indonesian fruit bats.

Year	Location	Bat species	Number of positive samples				
			Neutralizing antibody titer ($PRNT_{80}$)				
			1:20	1:80	1:320	1:1280	Total (%)
2010	Panjalu	*Pteropus vampyrus*	4	6	3	1	14/15 (93.3)
2011	Lima Puluh Kota	*Pteropus vampyrus*	1	6	3	0	10/10 (100)
	Paguyaman	*Pteropus* sp.[a]	6	5	2	3	16/18 (88.9)
	Popayato	*Pteropus* sp.	0	0	1	2	3/3 (100)
2012	Paguyaman	*Dobsonia moluccensis*	2	6	8	0	16/16 (100)
		Acerodon celebensis	6	2	0	0	8/18 (44.4)
		Pteropus sp.	2	0	0	0	2/2 (100)
	Surabaya	*Pteropus vampyrus*	1	0	0	2	3/3 (100)
	Magelang	*Pteropus vampyrus*	5	6	4	2	17/19 (89.5)
2013	Paguyaman	*Pteropus* sp.	0	7	2	0	9/10 (90)
		Acerodon celebensis	1	1	0	0	2/10 (20)
2014	Soppeng	*Pteropus* sp.	1	3	1	0	5/6 (83.3)
	Sidrap	*Pteropus* sp.	2	1	0	0	3/3 (100)
Total			**31**	**43**	**24**	**10**	**108/133 (81.2)**

554 [a]*Pteropus* sp.; Bat genetically closely related to *Pteropus hypomelanus*

555

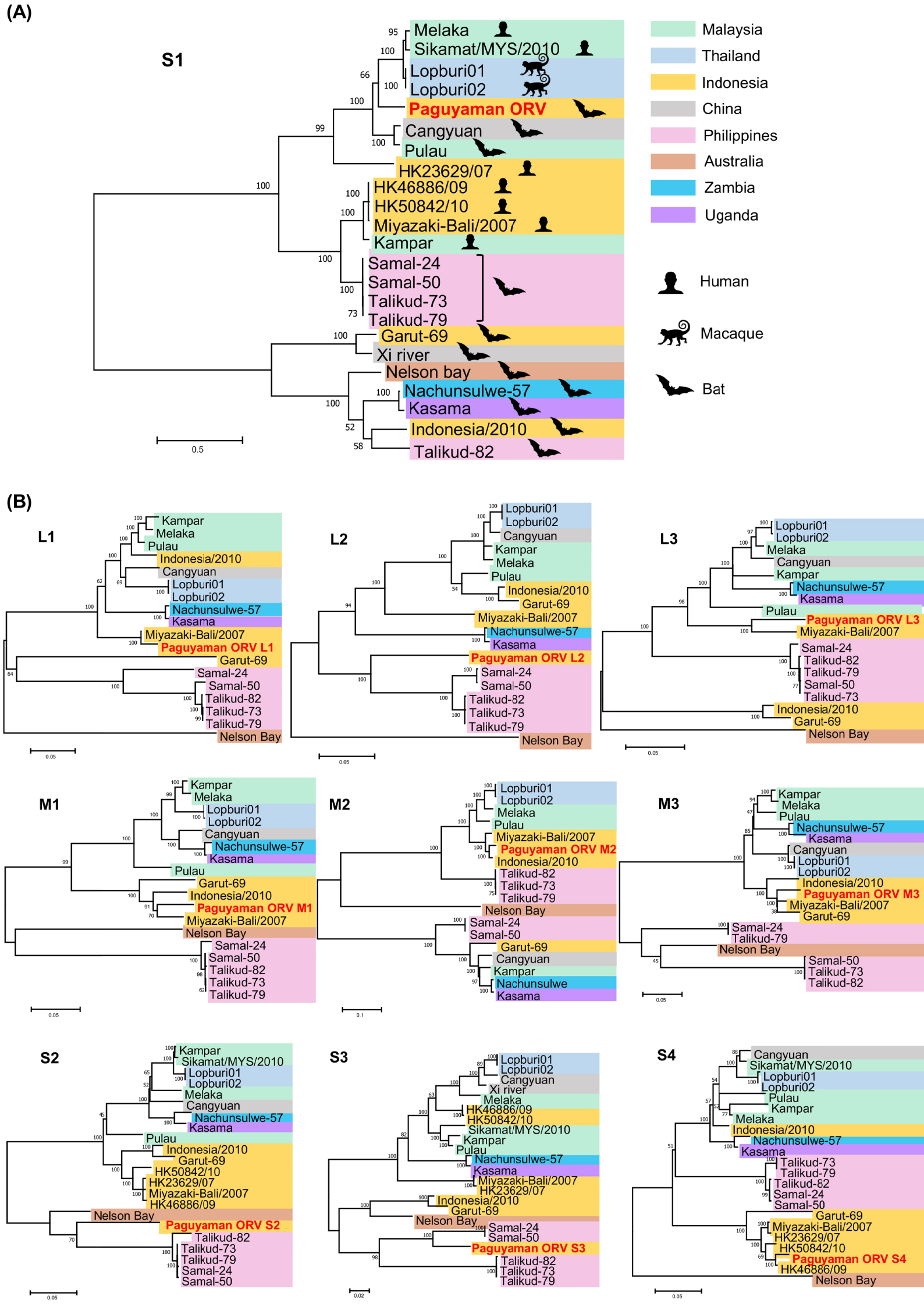
(A)
S1
Melaka
Sikamat/MYS/2010
Lopburi01
Lopburi02
Paguyaman ORV
Cangyuan
Pulau
HK23629/07
HK46886/09
HK50842/10
Miyazaki-Bali/2007
Kampar
Samal-24
Samal-50
Talikud-73
Talikud-79
Garut-69
Xi river
Nelson bay
Nachunsulwe-57
Kasama
Indonesia/2010
Talikud-82
0.5
Malaysia
Thailand
Indonesia
China
Philippines
Australia
Zambia
Uganda
Human
Macaque
Bat
(B)
L1
Kampar
Melaka
Pulau
Indonesia/2010
Cangyuan
Lopburi01
Lopburi02
Nachunsulwe-57
Kasama
Miyazaki-Bali/2007
Paguyaman ORV L1
Garut-69
Samal-24
Samal-50
Talikud-82
Talikud-73
Talikud-79
Nelson Bay
L2
Lopburi01
Lopburi02
Cangyuan
Kampar
Melaka
Pulau
Indonesia/2010
Garut-69
Miyazaki-Bali/2007
Nachunsulwe-57
Kasama
Paguyaman ORV L2
Samal-24
Samal-50
Talikud-82
Talikud-73
Talikud-79
Nelson Bay
L3
Lopburi01
Lopburi02
Melaka
Cangyuan
Kampar
Nachunsulwe-57
Kasama
Pulau
Paguyaman ORV L3
Miyazaki-Bali/2007
Samal-24
Talikud-82
Talikud-79
Samal-50
Talikud-73
Indonesia/2010
Garut-69
Nelson Bay
M1
Kampar
Melaka
Lopburi01
Lopburi02
Cangyuan
Nachunsulwe-57
Kasama
Pulau
Garut-69
Indonesia/2010
Paguyaman ORV M1
Miyazaki-Bali/2007
Nelson Bay
Samal-24
Samal-50
Talikud-82
Talikud-73
Talikud-79
M2
Lopburi01
Lopburi02
Melaka
Pulau
Miyazaki-Bali/2007
Paguyaman ORV M2
Indonesia/2010
Talikud-82
Talikud-73
Talikud-79
Nelson Bay
Samal-24
Samal-50
Garut-69
Cangyuan
Kampar
Nachunsulwe
Kasama
M3
Kampar
Melaka
Pulau
Nachunsulwe-57
Kasama
Cangyuan
Lopburi01
Lopburi02
Indonesia/2010
Paguyaman ORV M3
Miyazaki-Bali/2007
Garut-69
Samal-24
Talikud-79
Nelson Bay
Samal-50
Talikud-73
Talikud-82
S2
Kampar
Sikamat/MYS/2010
Lopburi01
Lopburi02
Melaka
Cangyuan
Nachunsulwe-57
Kasama
Pulau
Indonesia/2010
Garut-69
HK50842/10
HK23629/07
Miyazaki-Bali/2007
HK46886/09
Nelson Bay
Paguyaman ORV S2
Talikud-82
Talikud-73
Talikud-79
Samal-24
Samal-50
S3
Lopburi01
Lopburi02
Cangyuan
Xi river
Melaka
HK46886/09
HK50842/10
Sikamat/MYS/2010
Kampar
Pulau
Nachunsulwe-57
Kasama
Miyazaki-Bali/2007
HK23629/07
Indonesia/2010
Garut-69
Nelson Bay
Samal-24
Samal-50
Paguyaman ORV S3
Talikud-82
Talikud-73
Talikud-79
S4
Cangyuan
Sikamat/MYS/2010
Lopburi01
Lopburi02
Pulau
Kampar
Melaka
Indonesia/2010
Nachunsulwe-57
Kasama
Talikud-73
Talikud-79
Talikud-82
Samal-24
Samal-50
Garut-69
Miyazaki-Bali/2007
HK23629/07
HK50842/10
Paguyaman ORV S4
HK46886/09
Nelson Bay

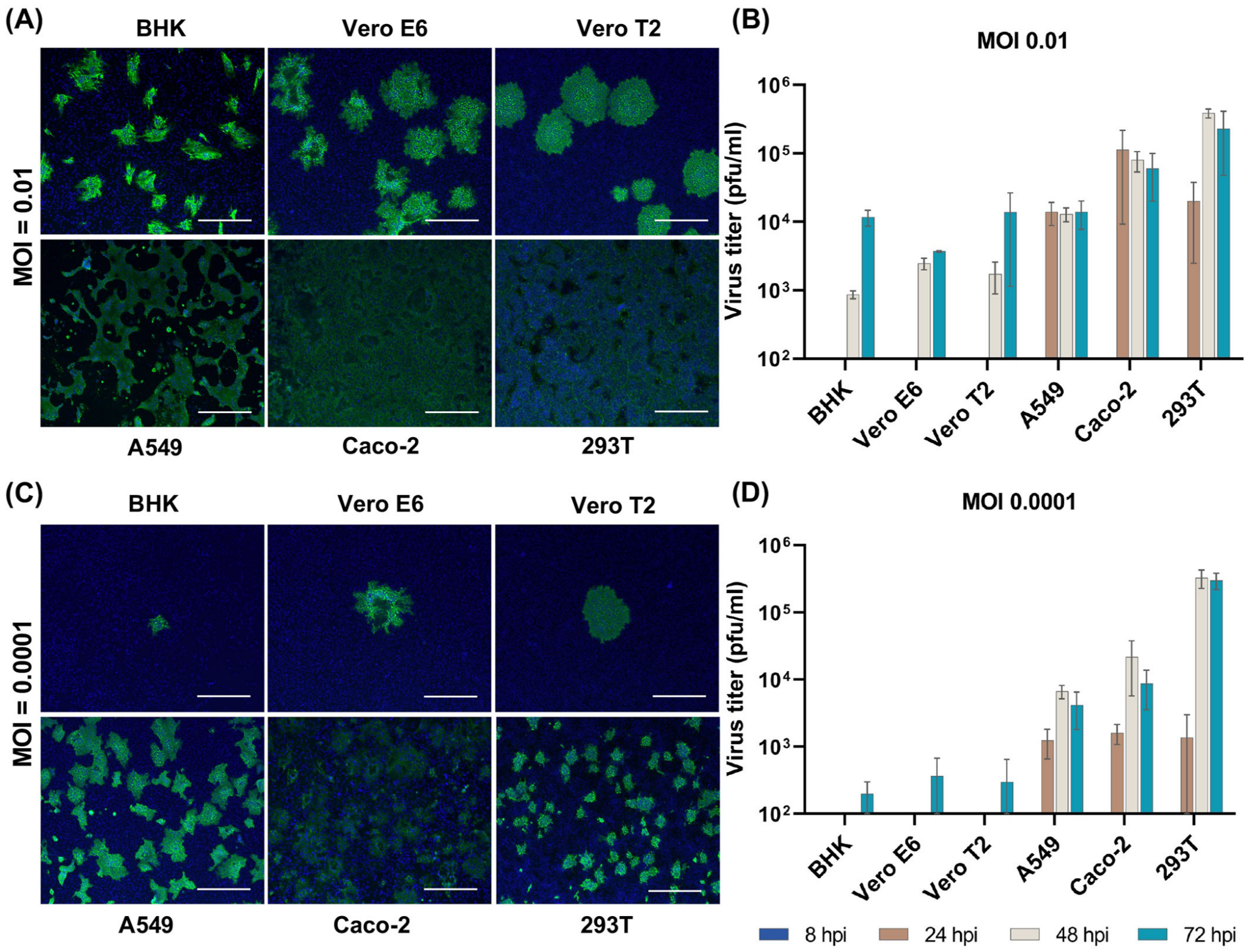
(A)
BHK
Vero E6
Vero T2
MOI = 0.01
A549
Caco-2
293T
(B)
MOI 0.01
Virus titer (pfu/ml)
10^6
10^5
10^4
10^3
10^2
BHK
Vero E6
Vero T2
A549
Caco-2
293T
(C)
BHK
Vero E6
Vero T2
MOI = 0.0001
A549
Caco-2
293T
(D)
MOI 0.0001
Virus titer (pfu/ml)
10^6
10^5
10^4
10^3
10^2
BHK
Vero E6
Vero T2
A549
Caco-2
293T
8 hpi
24 hpi
48 hpi
72 hpi

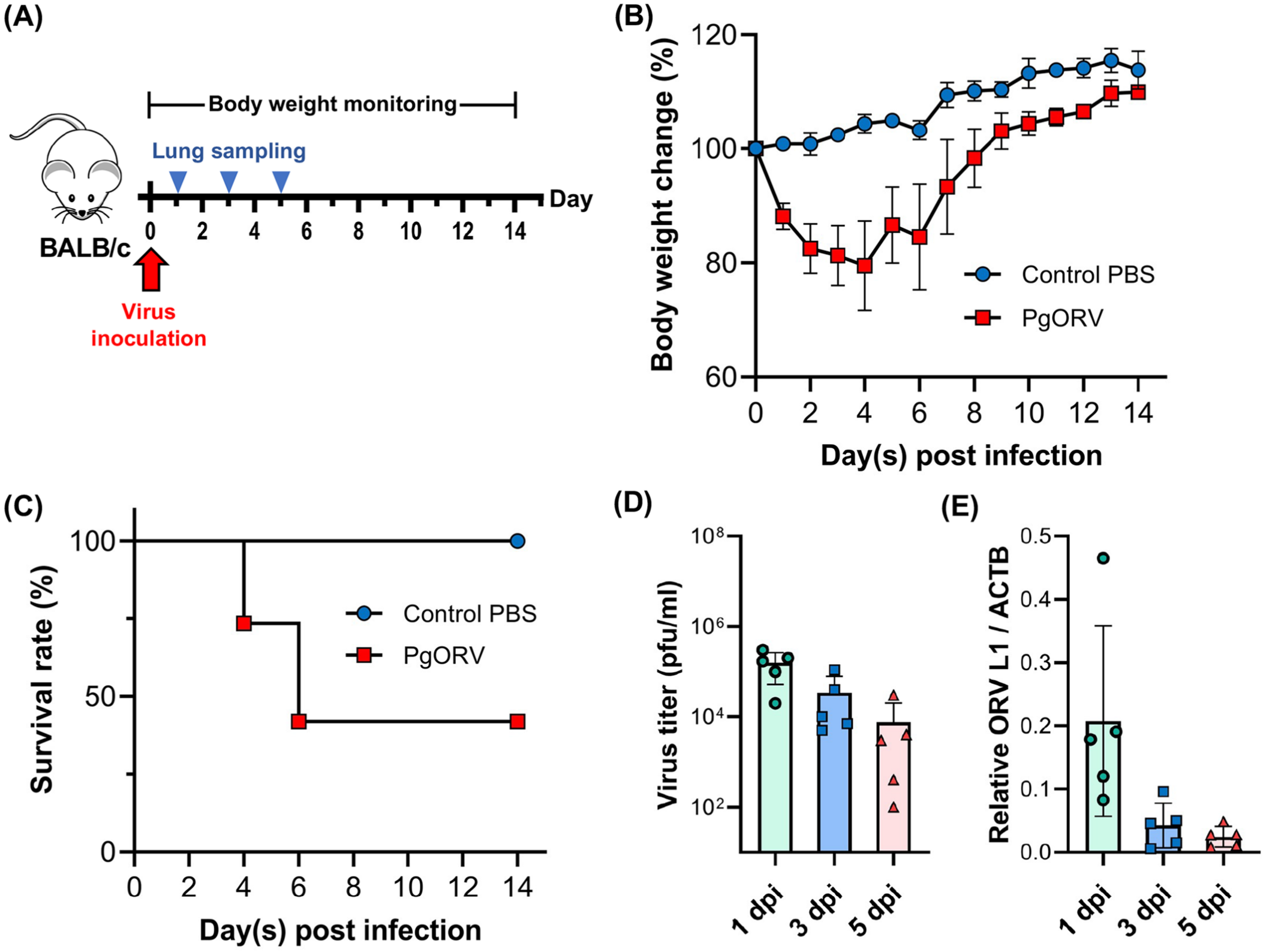
(A)
Body weight monitoring
Lung sampling
Day
0 2 4 6 8 10 12 14
BALB/c
Virus inoculation
(B)
Body weight change (%)
120
100
80
60
Control PBS
PgORV
0 2 4 6 8 10 12 14
Day(s) post infection
(C)
Survival rate (%)
100
50
0
Control PBS
PgORV
0 2 4 6 8 10 12 14
Day(s) post infection
(D)
Virus titer (pfu/ml)
10^8
10^6
10^4
10^2
1 dpi
3 dpi
5 dpi
(E)
Relative ORV L1 / ACTB
0.5
0.4
0.3
0.2
0.1
0.0
1 dpi
3 dpi
5 dpi

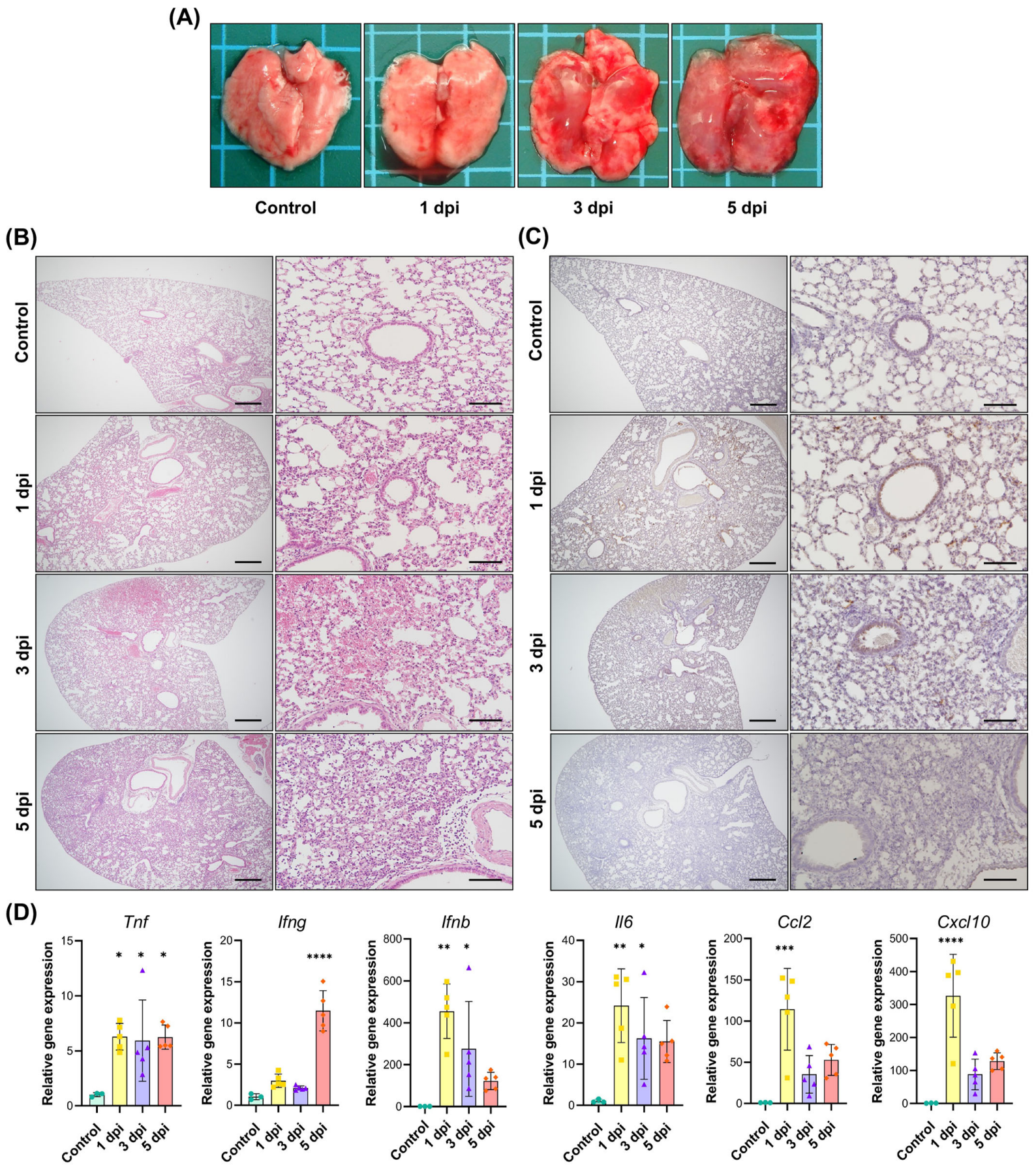
(A)
Control
1 dpi
3 dpi
5 dpi
(B)
(C)
Control
1 dpi
3 dpi
5 dpi
(D)
Tnf
Ifng
Ifnb
Il6
Ccl2
Cxcl10
Relative gene expression
Control
1 dpi
3 dpi
5 dpi